International Journal of Innovative
Computing, Information and Control
Volume **16**, Number **6**, December **2020**

 ISSN 1349-4198
pp. 1877–1894

NOVEL COOPERATIVE FPA-ATS ALGORITHM AND ITS APPLICATION TO OPTIMAL FOPID CONTROLLER DESIGN FOR LOAD FREQUENCY CONTROL

Thitipong Niyomsat and Deacha Puangdownreong

Department of Electrical Engineering
Southeast Asia University
19/1 Petchkasem Rd., Nongkhangphlu, Nonghkaem, Bangkok 10160, Thailand
deachap@sau.ac.th

Received June 2020; revised October 2020

Abstract. *This paper proposes a novel cooperative metaheuristic optimization algorithm for control system design optimization. The proposed algorithm denoted as the cooperative FPA-ATS is formed from the flower pollination algorithm (FPA), one of the most efficient population-based metaheuristic optimization techniques, and the adaptive tabu search (ATS), one of the most powerful trajectory-based metaheuristic optimization techniques. The cooperative FPA-ATS possesses two states running in a sequential manner as serial-heterogeneous search algorithms. It begins the search for the feasible solutions over entire search space by using the FPA's exploration property. Afterwards, it searches for the global solution by using the ATS's exploitation property. The search performance comparison studies of the ATS, FPA and the cooperative FPA-ATS are reported by testing against ten benchmark functions. As results, the cooperative FPA-ATS shows superiority to FPA and ATS, respectively. The cooperative FPA-ATS is then applied to designing the fractional-order proportional-integral derivative (FOPID) controller for the load frequency control (LFC) in power systems with three types of turbines. Based on the modern optimization, the cooperative FPA-ATS can provide optimal FOPID controllers for LFC systems. Once compared with the integer-order PID (IOPID) controller, the FOPID controller can yield very satisfactory response superior to the IOPID controller.*
Keywords: Cooperative FPA-ATS algorithm, Flower pollination algorithm, Adaptive tabu search, Fractional-order PID controller, Load frequency control

1. **Introduction.** Metaheuristic algorithms have been consecutively developed and widely applied to solving combinatorial and numeric optimization problems over three decades [1,2]. Ideal metaheuristic algorithm possesses two main properties, i.e., exploration (or diversification) and exploitation (or intensification). The explorative property is to generate diverse solutions to explore the search space on the global scale. The exploitative property is to focus on the search in a local region by exploiting the information to reach the best local solution within this region [1-5]. Many metaheuristic algorithms are consecutively proposed to perform their effectiveness. Based on the modern optimization, metaheuristic algorithms can be divided into two categories, i.e., trajectory-based (or single-solution based) and population-based metaheuristic algorithms. The trajectory-based metaheuristic algorithms have strong exploitative property, while the population-based metaheuristic algorithms have strong explorative characteristics [1,2].

Following the literature, the adaptive tabu search (ATS) is one of the most efficient trajectory-based metaheuristic algorithms. The ATS was firstly proposed by Sujitjorn and his colleagues in 2006 [6] based on the original tabu search (TS) proposed by Glover

DOI: 10.24507/ijicic.16.06.1877

in 1989 [7,8]. The ATS was widely applied to solving several real-world engineering problems including system identification [9-13], control system design [14-18], power systems [19-23] and signal processing [24]. Moreover, the global convergence properties of the ATS have been proved by the relevant probabilistic theory [25-27]. One of the most powerful population-based metaheuristic algorithms is the flower pollination algorithm (FPA) proposed by Yang in 2012 [28]. The FPA was successfully applied to solving many real-world engineering problems including power systems [29,30], signal and image processing [31,32], wireless sensor networking [33,34], traveling transportation [35], structural and mechanical engineering optimization [36,37] and control engineering problems [38-41]. In addition, the global convergence properties of the FPA algorithm have been proven by Markov chain theory [42].

Recently, the paradigm of the metaheuristic algorithms has been changed to balance the explorative and exploitative properties for searching performance improvement. A new paradigm for combinatorial optimization was proposed by Talbi [43]. The taxonomy of new-paradigm metaheuristic algorithms can be classified as parallel, hybrid and cooperative metaheuristic algorithms [43,44]. The parallel and hybrid metaheuristic algorithms are the former, while the cooperative metaheuristic algorithms are the later. The taxonomy of the cooperative metaheuristic algorithms based on the types of algorithms being used in the cooperative system and the implementation can be classified into four different categories [44], i.e., (1) serial-homogenous algorithms with same algorithms running in a sequential manner, (2) parallel-homogenous algorithms with same algorithms running in a parallel manner, (3) serial-heterogeneous algorithms with different algorithms running in a sequential manner and (4) parallel-heterogeneous algorithms with different algorithms running in parallel manner.

With the dominant exploitative property of the ATS and the dominant explorative property of the FPA, a novel cooperative FPA-ATS metaheuristic optimization algorithm is proposed in this paper as one of the serial-heterogeneous cooperative search algorithms. Due to its explorative property, the FPA will be firstly activated for searching an elite solution. Afterwards, the ATS will be secondly invoked by using the elite solution supplied by the FPA as an initial solution. With its exploitative property, the ATS will move towards the global solution very rapidly. The proposed cooperative FPA-ATS is then applied to controlling application for designing the FOPID controller of the load frequency control (LFC) used in power systems. This paper consists of six sections. After an introduction performed in Section 1, the ATS, FPA and the proposed cooperative FPA-ATS algorithms are described in Section 2. Performance evaluation of the cooperative FPA-ATS algorithms is reported in Section 3. Problem formulation of the cooperative FPA-ATS based FOPID controller design optimization for the LFC control systems is formulated in Section 4. Results and discussions are illustrated in Section 5. Finally, conclusions are given in Section 6.

2. **Cooperative FPA-ATS Algorithm.**

In this section, the ATS and FPA algorithms are briefly described. Then, the proposed cooperative FPA-ATS algorithms are illustrated.

2.1. **ATS algorithm.**

The ATS algorithm, one of the most powerful trajectory-based metaheuristic algorithms having the dominant exploitative property, is based on randomly iterative neighborhood search approach [6]. The feasible solution called neighborhood will be randomly generated within the search radius. The ATS algorithm consists of the tabu list (TL), adaptive-radius (AR) mechanism and back-tracking (BT) mechanism. Both AR and BT mechanisms are regarded as the aspiration criteria (AC). The TL is used to record the list of visited solutions along the search process. The AR mechanism is

conducted to speed up the search process by reducing the search radius. Once the local entrapment occurs by some local optima, the BT mechanism is activated by using some visited solutions recorded in the TL to escape from such the entrapment. The search will move to new search space in order to reach the global optimum. The ATS algorithm can be represented by the flow diagram as shown in Figure 1, where TC stands for the termination criteria.

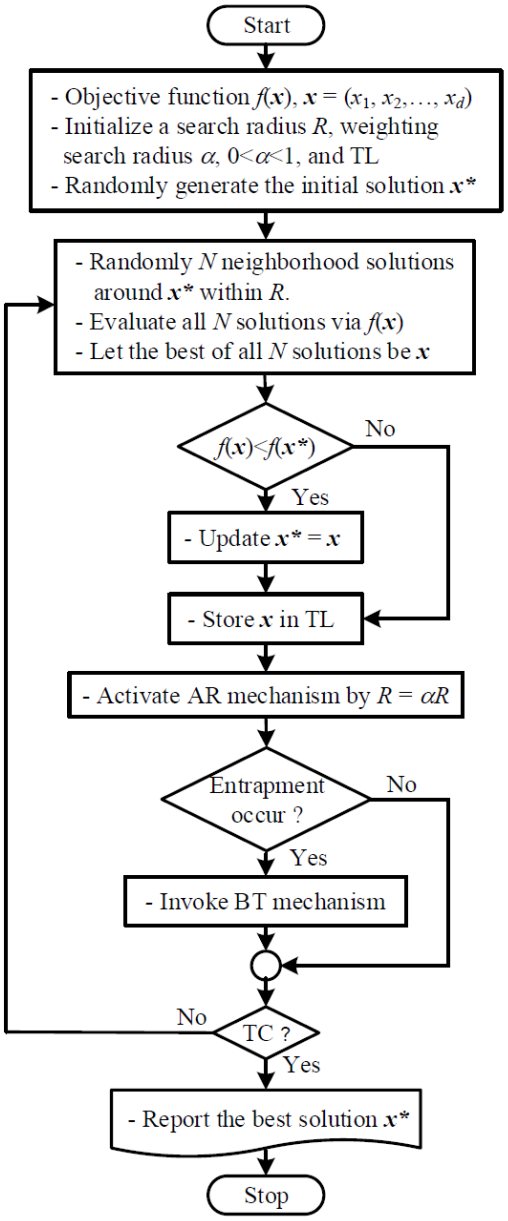

FIGURE 1. Flow diagram of the ATS

2.2. **FPA algorithm.** The FPA algorithm, one of the most efficient population-based metaheuristic algorithms having the dominant explorative property, mimics the pollination behavior of the flowering plants in nature. It can be divided into cross (or global) pollination and self (or local) pollination [28]. For the cross-pollination, pollen will be transferred by the biotic pollinator. In this case, the new position (or solution) $\boldsymbol{x}^{t+1}$ can be calculated by (1), where $\boldsymbol{x}^t$ is the current position, $\boldsymbol{g}^*$ is the current best solution, L is

the random drawn from Lévy flight distribution as stated in (2) and $\Gamma(\lambda)$ is the standard gamma function. For the self-pollination, pollen will be transferred by the abiotic pollinator. For this case, $\boldsymbol{x}^{t+1}$ can be calculated by (3), where ε is the random drawn from a uniform distribution as expressed in (4). A switch probability p is used for switching between cross-pollination and self-pollination. The FPA algorithm can be described by the flow diagram as shown in Figure 2.

$$\boldsymbol{x}_i^{t+1} = \boldsymbol{x}_i^t + L\left(\boldsymbol{x}_i^t - \boldsymbol{g}^*\right) \tag{1}$$

$$L \approx \frac{\lambda\Gamma(\lambda)\sin(\pi\lambda/2)}{\pi}\frac{1}{s^{1+\lambda}}, \quad (s \gg s_0 > 0) \tag{2}$$

$$\boldsymbol{x}_i^{t+1} = \boldsymbol{x}_i^t + \varepsilon\left(\boldsymbol{x}_j^t - \boldsymbol{x}_k^t\right) \tag{3}$$

$$\varepsilon(\rho) = \begin{cases} 1/(b-a), & a \le \rho \le b \\ 0, & \rho < a \text{ or } \rho > b \end{cases} \tag{4}$$

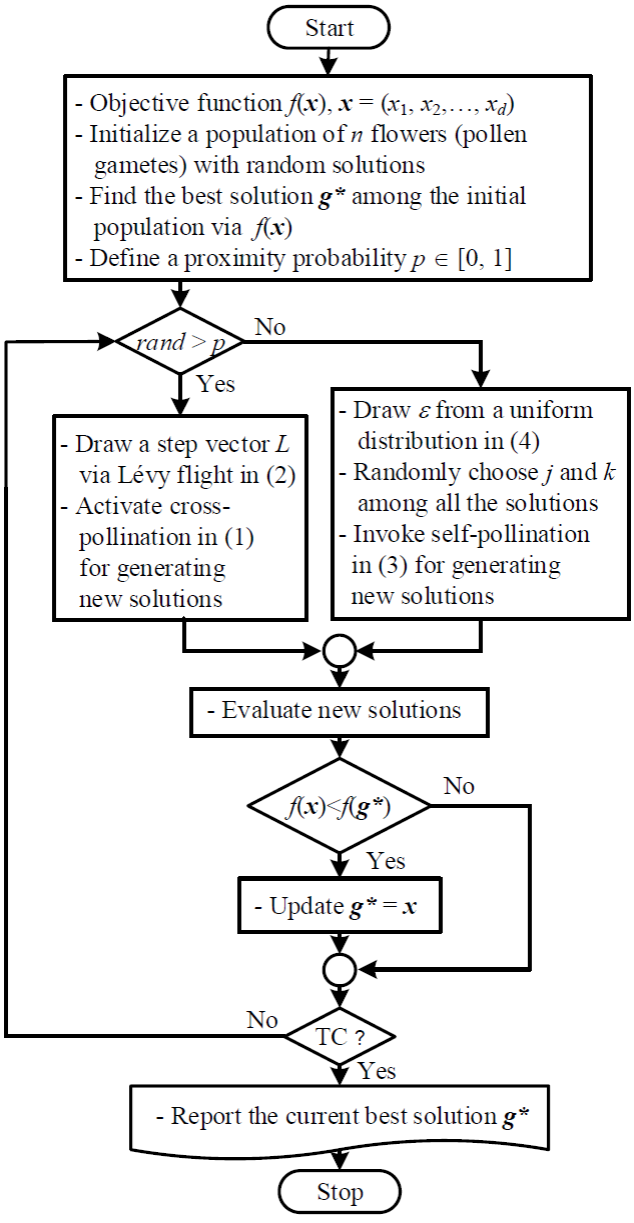

FIGURE 2. Flow diagram of the FPA

2.3. **Cooperative FPA-ATS algorithm.** The cooperative FPA-ATS algorithm is proposed by using the ATS and FPA algorithms running in the serial-heterogeneous cooperative manner. The cooperative FPA-ATS algorithm possesses two states for sequential cooperation. For the first stage, the FPA algorithm as shown in Figure 2 will be activated to explore the elite feasible solutions over entire search space with its explorative property. For the second stage, the ATS algorithm shown in Figure 1 will be invoked by using the elite solution supplied from the FPA as an initial solution to rapidly reach the global solution with its exploitative property. Such two states of the FPA-ATS can be divided by the switching generation (SG). Setting the SG setting depends on the problems of interest. The more the local optima of the problem are (close to high multi-modal), the more the SG value is set. On the other hand, the less the local optima of the problem are (close to unimodal), the less the SG value is defined. For the normal case, the SG value can be set as the half value of the maximum generation. From literature reviews [43,44], the cooperative FPA-ATS algorithm proposed in this paper differs from other cooperative algorithms in that the proposed cooperative FPA-ATS algorithm utilizes two of the most efficient algorithms having different property, i.e., ATS having strong exploitative property and FPA having strong explorative property, for searching the global optimum in the serial-heterogeneous cooperative manner. The proposed cooperative FPA-ATS algorithm can be represented by the flow diagram as shown in Figure 3.

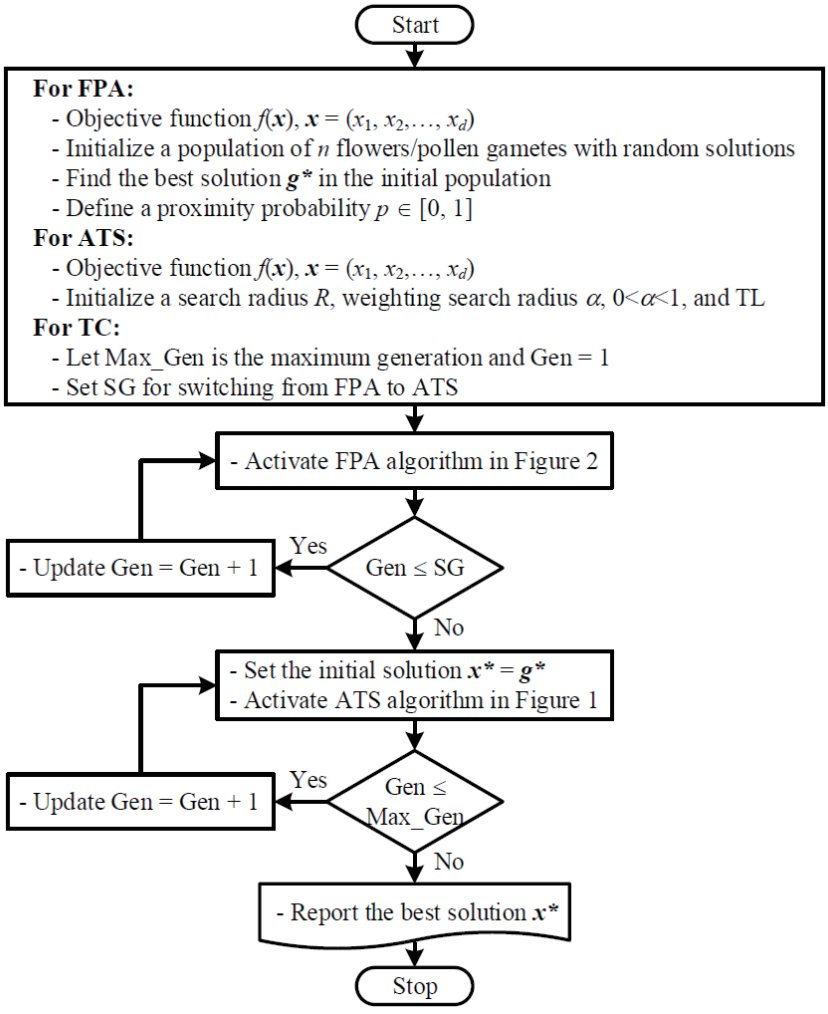

FIGURE 3. Flow diagram of the proposed cooperative FPA-ATS

3. **Performance Evaluation of Cooperative FPA-ATS.** In order to perform its search performance, the proposed cooperative FPA-ATS will be tested against 10 selected benchmark functions [45,46] as summarized in Table 1. For the performance evaluation and comparison, the ATS, FPA and cooperative FPA-ATS algorithms were coded by MATLAB version 2017b (License No.#40637337). Searching parameters of the ATS are set according to recommendations [6] and the preliminary study as shown in Table 2. Those of the FPA are set according to recommendations [28] and the preliminary study for all benchmark functions. The preliminary study of the FPA for all selected benchmark functions is done by varying numbers of flowers n = 5, 10, 15, 20, 25, 30, 40, 50, 75, 100, 150, 250, 500 and 1,000 and a switch probability p = 0.00, 0.01, 0.05, 0.10, 0.15, 0.20, 0.25, 0.30, 0.35, 0.40, 0.45, 0.50, 0.55, 0.60, 0.65, 0.70, 0.75, 0.80, 0.85, 0.90, 0.95 and 1.00. From results of the preliminary study, the optimal parameters of the FPA for all benchmark functions are n = 15-25 and p = 0.2-0.75. In this evaluation test, n = 20 and p = 0.5 are set for all benchmark functions. Searching parameters of the cooperative FPA-ATS algorithm are set according to the preliminary study as summarized in Table 3. 100 trial runs are conducted for each algorithm. All algorithms will be terminated once two termination criteria (TC) are satisfied, i.e., (1) the function values are less than a given tolerance $\varepsilon \leq 10^{-5}$ or (2) the search meets the maximum generation (Max_Gen = 1,000). The former criterion implies that the search is success, while the later means that the search is not success.

The comparison results between ATS, FPA and cooperative FPA-ATS are summarized in Table 4. The numeric data in Table 4 are presented in the following format, i.e., AE±SD(SR%), where the AE is the average number (mean) of function evaluations, the SD is the standard deviation and the SR is the success rate. The AE value implies the searching time consumed. The less the AE, the less the searching time consumed. The SD value implies the robustness of the algorithm. The less the SD, the more the robustness. From Table 4, the proposed cooperative FPA-ATS yields more efficiency in finding the global minima of all selected benchmark functions than the FPA and ATS, respectively, with the highest SR and smallest AE and SD values. This is because the cooperative FPA-ATS proposed in this work possesses both exploitative and explorative properties. From simulation results of performance evaluation, it can be noticed that the proposed cooperative FPA-ATS performs superiority to FPA and ATS for function minimization.

For example, movements and convergent rates of the cooperative FPA-ATS for global minimum finding of the Griewank function (GF) are plotted in Figure 4. It can be observed that the cooperative FPA-ATS can reach the global minima with the 1st TC for all trial runs.

4. **Problem Formulation of Cooperative FPA-ATS-Based FOPID Controller Design.** This section presents the problem formulation of the cooperative FPA-ATS-based FOPID controller design optimization for the LFC control systems. The considered LFC system, the FOPID controller and the problem formulation of the cooperative FPA-ATS-based FOPID controller design optimization are described as follows.

4.1. **LFC system.** In power generation systems, the LFC is one of the most important parts [47,48]. The LFC plays an important role to maintain the frequency of power systems with zero of the area control error (ACE). Also, it keeps tie-line power flows within some pre-defined tolerances. The LFC control models can be linearized and represented by a block diagram as shown in Figure 5, where $G_g(s)$, $G_t(s)$, $G_m(s)$ and $G_d(s)$ are linear models of governor, turbine, load-machine and droop dynamics, respectively. Referring to Figure 5, ΔP_d is load disturbance (p.u.MW), ΔP_G is an incremental change in governor

TABLE 1. Summary of ten selected benchmark functions

Benchmark functions	**Names, Functions, Search space, Coefficients, Optimal solutions ($\boldsymbol{x}^*$) and Optimal function values $f(\boldsymbol{x}^*)$**	**3D surfaces**
$f_1(\boldsymbol{x})$	Griewank function (GF) $f_1(\boldsymbol{x}) = \sum_{i=1}^{N} \frac{x_i^2}{4000} - \prod_{i=1}^{N} \cos\left(\frac{x_i}{\sqrt{i}}\right) + 1,$ $-100 \le x_1, x_2 \le 100,\ i = 1, 2,\ N = 2,$ $\boldsymbol{x}^* = (0, 0),\ f_1(\boldsymbol{x}^*) = 0$	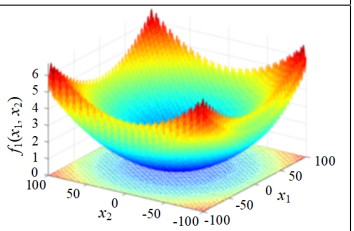
$f_2(\boldsymbol{x})$	Salomon function (SF) $f_2(\boldsymbol{x}) = 1 - \cos\left(2\pi\sqrt{\sum_{i=1}^{D} x_i^2}\right) + 0.1\sqrt{\sum_{i=1}^{D} x_i^2},$ $-4 \le x_1, x_2 \le 4,\ i = 1, 2,\ D = 2,$ $\boldsymbol{x}^* = (0, 0),\ f_2(\boldsymbol{x}^*) = 0$	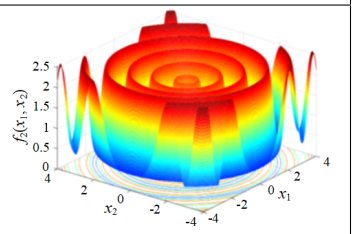
$f_3(\boldsymbol{x})$	Michaelwicz function (MF) $f_3(\boldsymbol{x}) = -\sum_{i=1}^{D} \sin(x_i) \sin^{2m}\left(\frac{ix_i^2}{\pi}\right),$ $0 \le x_1, x_2 \le \pi,\ i = 1, 2,\ m = 10,\ D = 2,$ $\boldsymbol{x}^* = (2.20, 1.57),\ f_3(\boldsymbol{x}^*) = -1.8013$	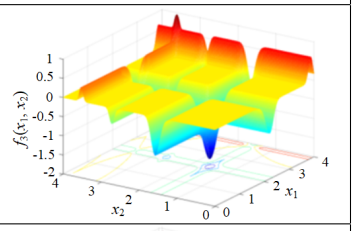
$f_4(\boldsymbol{x})$	Rastrigin function (RF) $f_4(\boldsymbol{x}) = 10D + \sum_{i=1}^{D} [x_i^2 - 10\cos(2\pi x_i)],$ $-5.12 \le x_1, x_2 \le 5.12,\ i = 1, 2,\ D = 2,$ $\boldsymbol{x}^* = (0, 0),\ f_4(\boldsymbol{x}^*) = 0$	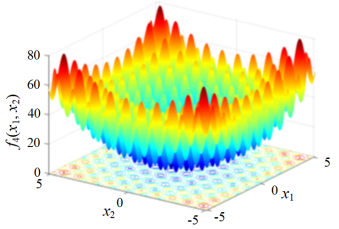
$f_5(\boldsymbol{x})$	Peaks function (PF) $f_5(\boldsymbol{x}) = 3(1 - x_1)^2 e^{[-x_1^2 - (x_2+1)^2]}$ $-10\left(\frac{x_1}{5} - x_1^3 - x_2^5\right) e^{(-x_1^2 - x_2^2)}$ $-\frac{1}{3} e^{[-(x_1+1)^2 - x_2^2]},$ $-4 \le x_1, x_2 \le 4,$ $\boldsymbol{x}^* = (0.2283, -1.6255),\ f_5(\boldsymbol{x}^*) = -6.5511$	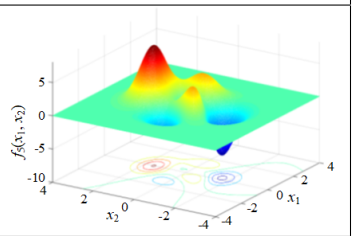
$f_6(\boldsymbol{x})$	Beale function (BF) $f_6(\boldsymbol{x}) = (1.5 - x_1 + x_1 x_2)^2 + (2.25 - x_1 + x_1 x_2^2)^2$ $+(2.625 - x_1 + x_1 x_2^3)^2,$ $-4.5 \le x_1, x_2 \le 4.5,$ $\boldsymbol{x}^* = (3, 0.5),\ f_6(\boldsymbol{x}^*) = 0$	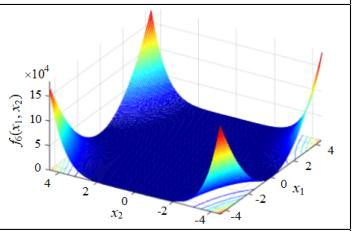
$f_7(\boldsymbol{x})$	Giunta function (GiF) $f_7(\boldsymbol{x}) = 0.6 + \sum_{i=1}^{2} \left[\sin\left(\frac{16}{15}x_i - 1\right)\right.$ $+\sin^2\left(\frac{16}{15}x_i - 1\right)$ $\left.+\frac{1}{50}\sin\left(4\left(\frac{16}{15}x_i - 1\right)\right)\right],$ $-1 \le x_1, x_2 \le 1,\ i = 1, 2,$ $\boldsymbol{x}^* = (0.46732, 0.46732),\ f_7(\boldsymbol{x}^*) = 0.06447$	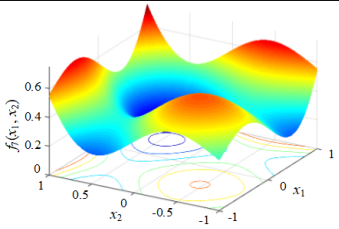

Continued

Continued

Benchmark functions	**Names, Functions, Search space, Coefficients, Optimal solutions ($\boldsymbol{x}^*$) and Optimal function values $f(\boldsymbol{x}^*)$**	**3D surfaces**
$f_8(\boldsymbol{x})$	Lévy function (LF) $f_8(\boldsymbol{x}) = \sin^2(3\pi x_1) + (x_1-1)^2[1+\sin^2(3\pi x_2)]$ $+(x_2-1)^2[1+\sin^2(2\pi x_2)]$, $-10 \le x_1, x_2 \le 10$, $\boldsymbol{x}^* = (1,1)$, $f_8(\boldsymbol{x}^*) = 0$	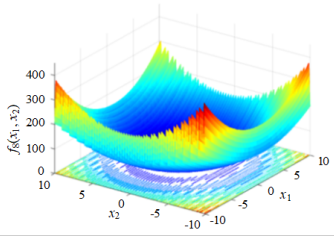
$f_9(\boldsymbol{x})$	Yang function (YF) $f_9(\boldsymbol{x}) = \left[e^{-\sum_{i=1}^{D}(x_i/\beta)^{2m}} - 2e^{-\sum_{i=1}^{D}(x_i-\pi)^2}\right.$ $\left. \cdot \prod_{i=1}^{D}\cos^2(x_i)\right]$, $-10 \le x_1, x_2 \le 10$, $m = 5$, $\beta = 15$, $i = 1,2$, $D = 2$, $\boldsymbol{x}^* = (\pi,\pi)$, $f_9(\boldsymbol{x}^*) = -1$	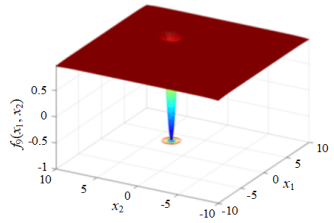
$f_{10}(\boldsymbol{x})$	Drop-Wave function (DWF) $f_{10}(\boldsymbol{x}) = -\frac{1+\cos\left(12\sqrt{x_1^2+x_2^2}\right)}{0.5(x_1^2+x_2^2)+2}$, $-5.12 \le x_1, x_2 \le 5.12$, $\boldsymbol{x}^* = (0,0)$, $f_{10}(\boldsymbol{x}^*) = -1$	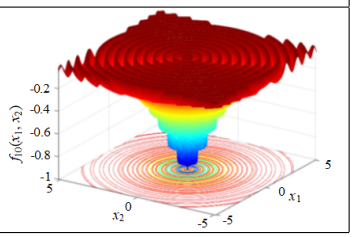

TABLE 2. Search parameters of the ATS

Benchmark functions	**Search parameters**					
	$\boldsymbol{N}$	$\boldsymbol{R}$(%)	$\boldsymbol{J}_{\max}$	**AR mechanism**		
				Stage-I	**Stage-II**	**Stage-III**
$f_1(\boldsymbol{x})$	30	20	15	$f(\boldsymbol{x}) < f(\boldsymbol{x}^*) + 1\text{e-}1$ $R = 1\text{e-}2$	$f(\boldsymbol{x}) < f(\boldsymbol{x}^*) + 1\text{e-}2$ $R = 1\text{e-}3$	$f(\boldsymbol{x}) < f(\boldsymbol{x}^*) + 1\text{e-}3$ $R = 1\text{e-}4$
$f_2(\boldsymbol{x})$	15	20	15	$f(\boldsymbol{x}) < f(\boldsymbol{x}^*) + 1\text{e-}1$ $R = 1\text{e-}2$	$f(\boldsymbol{x}) < f(\boldsymbol{x}^*) + 1\text{e-}2$ $R = 1\text{e-}3$	$f(\boldsymbol{x}) < f(\boldsymbol{x}^*) + 1\text{e-}3$ $R = 1\text{e-}4$
$f_3(\boldsymbol{x})$	20	20	15	$f(\boldsymbol{x}) < f(\boldsymbol{x}^*) + 1$ $R = 1\text{e-}2$	$f(\boldsymbol{x}) < f(\boldsymbol{x}^*) + 1\text{e-}1$ $R = 1\text{e-}3$	$f(\boldsymbol{x}) < f(\boldsymbol{x}^*) + 1\text{e-}2$ $R = 1\text{e-}4$
$f_4(\boldsymbol{x})$	20	20	15	$f(\boldsymbol{x}) < f(\boldsymbol{x}^*) + 1$ $R = 1\text{e-}2$	$f(\boldsymbol{x}) < f(\boldsymbol{x}^*) + 1\text{e-}1$ $R = 1\text{e-}3$	$f(\boldsymbol{x}) < f(\boldsymbol{x}^*) + 1\text{e-}2$ $R = 1\text{e-}4$
$f_5(\boldsymbol{x})$	25	20	15	$f(\boldsymbol{x}) < f(\boldsymbol{x}^*) + 1\text{e-}1$ $R = 1\text{e-}2$	$f(\boldsymbol{x}) < f(\boldsymbol{x}^*) + 1\text{e-}2$ $R = 1\text{e-}3$	$f(\boldsymbol{x}) < f(\boldsymbol{x}^*) + 1\text{e-}3$ $R = 1\text{e-}4$
$f_6(\boldsymbol{x})$	20	20	15	$f(\boldsymbol{x}) < f(\boldsymbol{x}^*) + 1\text{e-}2$ $R = 1\text{e-}2$	$f(\boldsymbol{x}) < f(\boldsymbol{x}^*) + 1\text{e-}3$ $R = 1\text{e-}3$	$f(\boldsymbol{x}) < f(\boldsymbol{x}^*) + 1\text{e-}4$ $R = 1\text{e-}4$
$f_7(\boldsymbol{x})$	20	20	15	$f(\boldsymbol{x}) < f(\boldsymbol{x}^*) + 1\text{e-}2$ $R = 1\text{e-}2$	$f(\boldsymbol{x}) < f(\boldsymbol{x}^*) + 1\text{e-}3$ $R = 1\text{e-}3$	$f(\boldsymbol{x}) < f(\boldsymbol{x}^*) + 1\text{e-}4$ $R = 1\text{e-}4$
$f_8(\boldsymbol{x})$	20	20	15	$f(\boldsymbol{x}) < f(\boldsymbol{x}^*) + 1\text{e-}1$ $R = 1\text{e-}2$	$f(\boldsymbol{x}) < f(\boldsymbol{x}^*) + 1\text{e-}2$ $R = 1\text{e-}3$	$f(\boldsymbol{x}) < f(\boldsymbol{x}^*) + 1\text{e-}3$ $R = 1\text{e-}4$
$f_9(\boldsymbol{x})$	20	20	15	$f(\boldsymbol{x}) < f(\boldsymbol{x}^*) + 1\text{e-}1$ $R = 1\text{e-}2$	$f(\boldsymbol{x}) < f(\boldsymbol{x}^*) + 1\text{e-}2$ $R = 1\text{e-}3$	$f(\boldsymbol{x}) < f(\boldsymbol{x}^*) + 1\text{e-}3$ $R = 1\text{e-}4$
$f_{10}(\boldsymbol{x})$	50	20	15	$f(\boldsymbol{x}) < f(\boldsymbol{x}^*) + 1\text{e-}1$ $R = 1\text{e-}2$	$f(\boldsymbol{x}) < f(\boldsymbol{x}^*) + 1\text{e-}2$ $R = 1\text{e-}3$	$f(\boldsymbol{x}) < f(\boldsymbol{x}^*) + 1\text{e-}3$ $R = 1\text{e-}4$

Note: N is numbers of neighborhood members,
R is an initial search radius (% = percentage of search space) and
$J_{\max}$ is number of maximum solution cycling to activate BT mechanism.

TABLE 3. Search parameters of the cooperative FPA-ATS

Benchmark functions	Search parameters of FPA-ATS								
	FPA		ATS						SG
						AR mechanism			
	n	p	N	R(%)	$J_{\max}$	Stage-I	Stage-II	Stage-III	
$f_1(\boldsymbol{x})$	20	0.5	5	20	5	$f(\boldsymbol{x}) < f(\boldsymbol{x}^*) + 1\text{e-}1$ $R = 1\text{e-}2$	$f(\boldsymbol{x}) < f(\boldsymbol{x}^*) + 1\text{e-}2$ $R = 1\text{e-}3$	$f(\boldsymbol{x}) < f(\boldsymbol{x}^*) + 1\text{e-}3$ $R = 1\text{e-}4$	700
$f_2(\boldsymbol{x})$	20	0.5	5	20	5	$f(\boldsymbol{x}) < f(\boldsymbol{x}^*) + 1\text{e-}1$ $R = 1\text{e-}2$	$f(\boldsymbol{x}) < f(\boldsymbol{x}^*) + 1\text{e-}2$ $R = 1\text{e-}3$	$f(\boldsymbol{x}) < f(\boldsymbol{x}^*) + 1\text{e-}3$ $R = 1\text{e-}4$	650
$f_3(\boldsymbol{x})$	20	0.5	5	20	5	$f(\boldsymbol{x}) < f(\boldsymbol{x}^*) + 1$ $R = 1\text{e-}2$	$f(\boldsymbol{x}) < f(\boldsymbol{x}^*) + 1\text{e-}1$ $R = 1\text{e-}3$	$f(\boldsymbol{x}) < f(\boldsymbol{x}^*) + 1\text{e-}2$ $R = 1\text{e-}4$	450
$f_4(\boldsymbol{x})$	20	0.5	5	20	5	$f(\boldsymbol{x}) < f(\boldsymbol{x}^*) + 1$ $R = 1\text{e-}2$	$f(\boldsymbol{x}) < f(\boldsymbol{x}^*) + 1\text{e-}1$ $R = 1\text{e-}3$	$f(\boldsymbol{x}) < f(\boldsymbol{x}^*) + 1\text{e-}2$ $R = 1\text{e-}4$	500
$f_5(\boldsymbol{x})$	20	0.5	5	20	5	$f(\boldsymbol{x}) < f(\boldsymbol{x}^*) + 1\text{e-}1$ $R = 1\text{e-}2$	$f(\boldsymbol{x}) < f(\boldsymbol{x}^*) + 1\text{e-}2$ $R = 1\text{e-}3$	$f(\boldsymbol{x}) < f(\boldsymbol{x}^*) + 1\text{e-}3$ $R = 1\text{e-}4$	400
$f_6(\boldsymbol{x})$	20	0.5	5	20	5	$f(\boldsymbol{x}) < f(\boldsymbol{x}^*) + 1\text{e-}2$ $R = 1\text{e-}2$	$f(\boldsymbol{x}) < f(\boldsymbol{x}^*) + 1\text{e-}3$ $R = 1\text{e-}3$	$f(\boldsymbol{x}) < f(\boldsymbol{x}^*) + 1\text{e-}4$ $R = 1\text{e-}4$	350
$f_7(\boldsymbol{x})$	20	0.5	5	20	5	$f(\boldsymbol{x}) < f(\boldsymbol{x}^*) + 1\text{e-}2$ $R = 1\text{e-}2$	$f(\boldsymbol{x}) < f(\boldsymbol{x}^*) + 1\text{e-}3$ $R = 1\text{e-}3$	$f(\boldsymbol{x}) < f(\boldsymbol{x}^*) + 1\text{e-}4$ $R = 1\text{e-}4$	350
$f_8(\boldsymbol{x})$	20	0.5	5	20	5	$f(\boldsymbol{x}) < f(\boldsymbol{x}^*) + 1\text{e-}1$ $R = 1\text{e-}2$	$f(\boldsymbol{x}) < f(\boldsymbol{x}^*) + 1\text{e-}2$ $R = 1\text{e-}3$	$f(\boldsymbol{x}) < f(\boldsymbol{x}^*) + 1\text{e-}3$ $R = 1\text{e-}4$	750
$f_9(\boldsymbol{x})$	20	0.5	5	20	5	$f(\boldsymbol{x}) < f(\boldsymbol{x}^*) + 1\text{e-}1$ $R = 1\text{e-}2$	$f(\boldsymbol{x}) < f(\boldsymbol{x}^*) + 1\text{e-}2$ $R = 1\text{e-}3$	$f(\boldsymbol{x}) < f(\boldsymbol{x}^*) + 1\text{e-}3$ $R = 1\text{e-}4$	700
$f_{10}(\boldsymbol{x})$	20	0.5	5	20	5	$f(\boldsymbol{x}) < f(\boldsymbol{x}^*) + 1\text{e-}1$ $R = 1\text{e-}2$	$f(\boldsymbol{x}) < f(\boldsymbol{x}^*) + 1\text{e-}2$ $R = 1\text{e-}3$	$f(\boldsymbol{x}) < f(\boldsymbol{x}^*) + 1\text{e-}3$ $R = 1\text{e-}4$	750

Note: n is number of flowers, p is a switch probability and SG is a switching generation.

TABLE 4. Results of performance evaluation of the ATS, FPA and cooperative FPA-ATS

Benchmark functions	Algorithms		
	ATS	FPA	Cooperative FPA-ATS
$f_1(\boldsymbol{x})$	2.6084e+4±8.7863e+3(19%)	1.9144e+4±2.1493e+3(25%)	1.8087e+4±4.3857e+1(100%)
$f_2(\boldsymbol{x})$	1.9372e+4±1.2604e+3(33%)	8.4843e+3±5.9445e+3(64%)	1.2759e+4±5.7823e+2(94%)
$f_3(\boldsymbol{x})$	8.1060e+3±8.4323e+3(69%)	4.4060e+3±8.9039e+2(100%)	2.4541e+3±7.0087e+2(100%)
$f_4(\boldsymbol{x})$	6.6418e+4±5.6778e+3(93%)	1.1531e+4±1.5912e+3(100%)	1.0104e+4±6.2667e+1(100%)
$f_5(\boldsymbol{x})$	3.5828e+3±7.0922e+2(100%)	2.4063e+3±2.0124e+2(100%)	2.0959e+3±2.8404e+1(100%)
$f_6(\boldsymbol{x})$	5.2738e+3±4.8956e+3(97%)	4.2318e+3±7.7897e+2(100%)	2.2692e+3±2.5601e+2(100%)
$f_7(\boldsymbol{x})$	2.2180e+3±6.7447e+2(100%)	2.0126e+3±6.1157e+2(100%)	1.9032e+3±6.4211e+1(100%)
$f_8(\boldsymbol{x})$	1.2386e+4±7.3786e+3(64%)	4.8612e+3±8.2381e+2(100%)	4.1518e+3±2.2803e+2(100%)
$f_9(\boldsymbol{x})$	8.3046e+3±4.2036e+3(93%)	4.8872e+3±4.3508e+3(98%)	1.8066e+4±9.4353e+1(99%)
$f_{10}(\boldsymbol{x})$	3.8454e+4±1.7935e+4(37%)	1.3988e+4±2.8423e+3(96%)	8.0852e+3±4.8977e+1(100%)

output (p.u.MW), ΔX_G is an incremental change in governor valve position, u is control signal input and Δf is an incremental frequency deviation output (Hz).

Models of $G_g(s)$, $G_m(s)$ and $G_d(s)$ are expressed in (5), (6) and (7), respectively, where T_g is time constant of governor, T_m is time constant of load-machine, K_m is load-machine gain and R is inverse droop gain [49].

$$G_g(s) = \frac{1}{T_g s + 1} \tag{5}$$

$$G_m(s) = \frac{K_m}{T_m s + 1} \tag{6}$$

$$G_d(s) = \frac{1}{R} \tag{7}$$

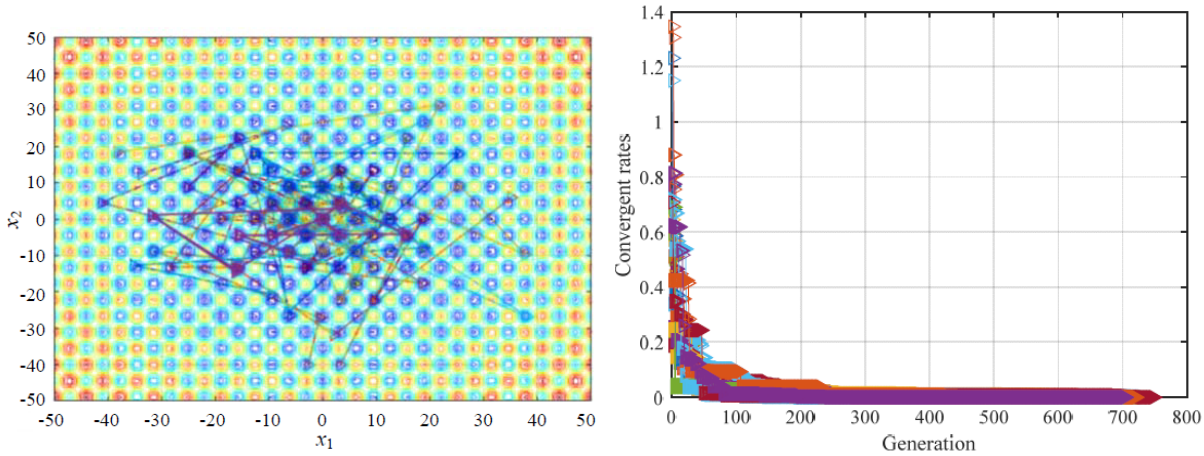

(a) Search movement (b) Convergent rates

FIGURE 4. Results of minimum finding of GF by cooperative FPA-ATS

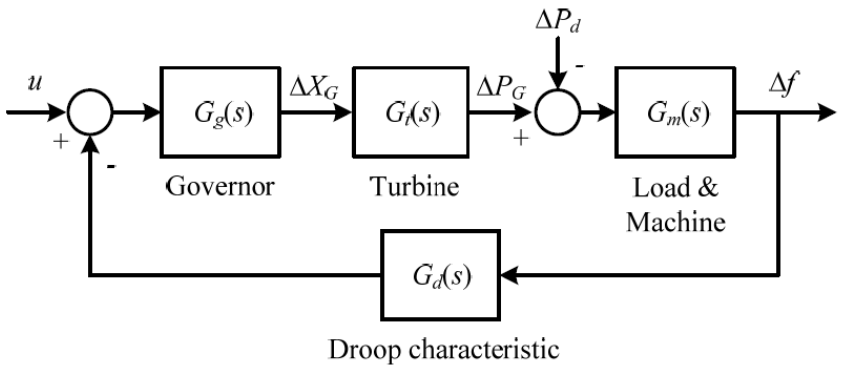

FIGURE 5. LFC control loop

In this work, three types of turbines including non-reheated, reheated and hydro turbines are conducted. The turbine models, $G_t(s)$, in (8), (9) and (10) are the non-reheated, reheated and hydro turbines, respectively, where T_t is time constant of turbine, T_r is a time constant of reheated turbine, c is the portion (percentage) of the power generated by the reheated process in the total generated power and T_h is a time constant of hydro turbine [49].

$$G_t^{non\text{-}reheated}(s) = \frac{1}{T_t s + 1} \tag{8}$$

$$G_t^{reheated}(s) = \frac{cT_r s + 1}{(T_r s + 1)(T_t s + 1)} \tag{9}$$

$$G_t^{hydro}(s) = \frac{1 - T_h s}{1 + 0.5 T_h s} \tag{10}$$

4.2. **FOPID controller.** Based on the traditional calculus, the time-domain and s-domain models of the conventional IOPID controller are stated in (11) and (12), where $e(t)$ is error signal regarded as the controller input and $u(t)$ is control signal regarded as the controller output, K_p is the proportional gain, K_i is the integral gain and K_d is the derivative gain. From (12), it was known that the IOPID controller has the integer-order with three parameters, i.e., K_p, K_i and K_d [50]. For the FOPID controller firstly

proposed by Podlubny in 1994 [51,52] based on the fractional calculus, the time-domain and s-domain models of the FOPID are given in (13) and (14), where D^{α} is non-integer order integro-differential operator and $\alpha \in \Re$ is the order of operation, $\lambda \in \Re$ is the fractional-order of the integral element and $\mu \in \Re$ is the fractional-order of the derivative element. From (14), it was found that the FOPID controller has the fractional-order with five parameters, i.e., K_p, K_i, K_d, λ and μ.

$$u(t)|_{IOPID} = K_p e(t) + K_i \int_0^t e(t)dt + K_d \frac{de(t)}{dt} \tag{11}$$

$$G_c(s)|_{IOPID} = K_p + \frac{K_i}{s} + K_d s \tag{12}$$

$$u(t)|_{FOPID} = K_p e(t) + K_i D^{-\lambda} e(t) + K_d D^{\mu} e(t) \tag{13}$$

$$G_c(s)|_{FOPID} = K_p + \frac{K_i}{s^{\lambda}} + K_d s^{\mu} \tag{14}$$

4.3. **Cooperative FPA-ATS-based FOPID controller design optimization.** Based on the modern optimization, the cooperative FPA-ATS-based FOPID design optimization for the LFC systems can be represented by a block diagram as shown in Figure 6. The conducted framework is adapted from the controller design optimization frameworks [53-57]. Referring to Figure 6, once zero-input reference ($r = 0$) is assumed, the absolute value of $\Delta f(|\Delta f|)$ is set as the objective function. The objective function $|\Delta f|$ will be fed back to the cooperative FPA-ATS in order to be minimized by searching for the appropriated values of the FOPID parameters (K_p, K_i, K_d, λ and μ) corresponding to their search spaces and inequality constrained functions as expressed in (15), where $K_{p\_\min}$ and $K_{p\_\max}$ are search bounds of K_p, $K_{i\_\min}$ and $K_{i\_\max}$ are search bounds of K_i, $K_{d\_\min}$ and $K_{d\_\max}$ are search bounds of K_d, $\lambda_{\min}$ and $\lambda_{\max}$ are search bounds of λ, $\mu_{\min}$ and $\mu_{\max}$ are search bounds of μ, PO_{reg} is percent overshoot of regulation, $PO_{reg\_\max}$ is maximum allowance of PO_{reg}, t_{reg} is recovering time, $t_{reg\_\max}$ is maximum allowance of t_{reg}, e_{ss} is steady-state error and $e_{ss\_\max}$ is maximum allowance of e_{ss}. Once Δf of the power machine is varied and disturbed due to the load changing, it will affect the protection devices and overall system efficiency. $|\Delta f|$ which is set as the objective function in (15) will be minimized and regulated during operation. For the constrained functions in (15), they are set by the desired time-domain specification including PO_{reg}, t_{reg} and e_{ss}. Setting these constrained functions needs to meet both design specification limited by $PO_{reg\_\max}$, $t_{reg\_\max}$ and $e_{ss\_\max}$ and controller realization limited by $[K_{p\_\min}, K_{p\_\max}]$ for K_p, $[K_{i\_\min}, K_{i\_\max}]$ for K_i, $[K_{d\_\min}, K_{d\_\max}]$ for K_d, $[\lambda_{\min}, \lambda_{\max}]$ for λ and $[\mu_{\min}, \mu_{\max}]$ for μ, respectively.

$$\left.\begin{array}{ll} \textbf{Minimize} & f(K_p, K_i, K_d, \lambda, \mu) = |\Delta f| \\ \text{Subject to} & K_{p\_\min} \le K_p \le K_{p\_\max},\ K_{i\_\min} \le K_i \le K_{i\_\max}, \\ & K_{d\_\min} \le K_d \le K_{d\_\max},\ \lambda_{\min} \le \lambda \le \lambda_{\max}, \\ & \mu_{\min} \le \mu \le \mu_{\max},\ PO_{reg} \le PO_{reg\_\max}, \\ & t_{reg} \le t_{reg\_\max},\ e_{ss} \le e_{ss\_\max} \end{array}\right\} \tag{15}$$

5. **Results and Discussions.** To design the FOPID controller for the considered LFC control systems with three types of turbines (non-reheated, reheated and hydro turbines), the cooperative FPA-ATS algorithm was coded by MATLAB version 2017b (License No.#40637337) with FOMCON toolbox [58]. For all three cases of turbines, the search parameters of the cooperative FPA-ATS are set from the preliminary study, i.e., $n = 20$,

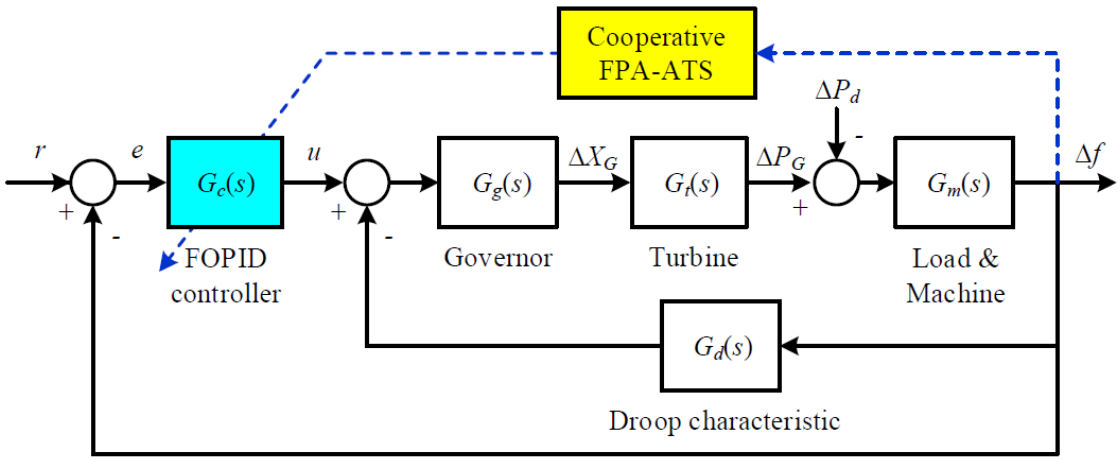

FIGURE 6. Cooperative FPA-ATS based FOPID controller design optimization for LFC

$p = 0.5$, $N = 5$, $R = 20\%$ of search bounds and $J_{\max} = 5$. In the AR mechanism, Stage-I: if $\Delta f <$ 1e-2, $R =$ 1e-2, Stage-II: if $\Delta f <$ 1e-3, $R =$ 1e-3 and Stage-III: if $\Delta f <$ 1e-4, R = 1e-4. Max_Gen = 200 is set as the TC of each trial run. To find the optimal FOPID controller parameters (K_p, K_i, K_d, λ and μ), 50 trial runs are conducted. For comparison with the IOPID controller, $\lambda = 1.0$ and $\mu = 1.0$ are assumed during the search process. The inequality constrained functions and search bounds in (15) are defined from the preliminary studies as expressed in (16).

$$\left.\begin{array}{ll} \textbf{Minimize} & \Delta f(K_p, K_i, K_d, \lambda, \mu) \\ \text{Subject to} & -20 \le K_p \le 20,\ 0 \le K_i \le 10, \\ & 0 \le K_d \le 5,\ 0.001 \le \lambda \le 1.0, \\ & 0.001 \le \mu \le 1.0,\ PO_{reg} \le 2.0\%, \\ & t_{reg} \le 50 \text{ s},\ e_{ss} \le 0.01\% \end{array}\right\} \tag{16}$$

5.1. **Case-I: LFC with non-reheated turbine.** For a non-reheated turbine, the model parameters are conducted as follows [49]: $K_m = 120$, $T_m = 20$ s, $T_t = 0.3$ s, $T_g = 0.08$ s and $R = 2.4$. Referring to Figure 5, the plant model, $G_p(s)$, is stated in (17).

$$\begin{aligned} G_p(s)|_{non\text{-}reheated\text{-}turbine} &= \frac{G_g G_t G_m}{1 + (G_g G_t^{non\text{-}reheated} G_m)/R} \\ &= \frac{250}{s^3 + 15.88s^2 + 42.46s + 106.2} \end{aligned} \tag{17}$$

Based on the cooperative FPA-ATS design optimization, the IOPID and FOPID controllers for the LFC system with a non-reheated turbine are optimized as expressed in (18) and (19), respectively. The convergent rates of the objective functions associated with inequality constrained functions in (16) over 50 trial runs are depicted in Figure 7. Responses of the LFC controlled system with a non-reheated turbine once a load disturbance $\Delta P_d = 0.01$ p.u.MW is applied are plotted in Figure 8.

$$G_c(s)|_{IOPID} = 0.5214 + \frac{0.5448}{s} + 0.1845s \tag{18}$$

$$G_c(s)|_{FOPID} = 5.1224 + \frac{4.6348}{s^{0.9813}} + 2.8506s^{0.9857} \tag{19}$$

As can be observed from Figure 8, both IOPID and FOPID controllers can improve the damping of the LFC system with a non-reheated turbine. Results obtained for case-I are

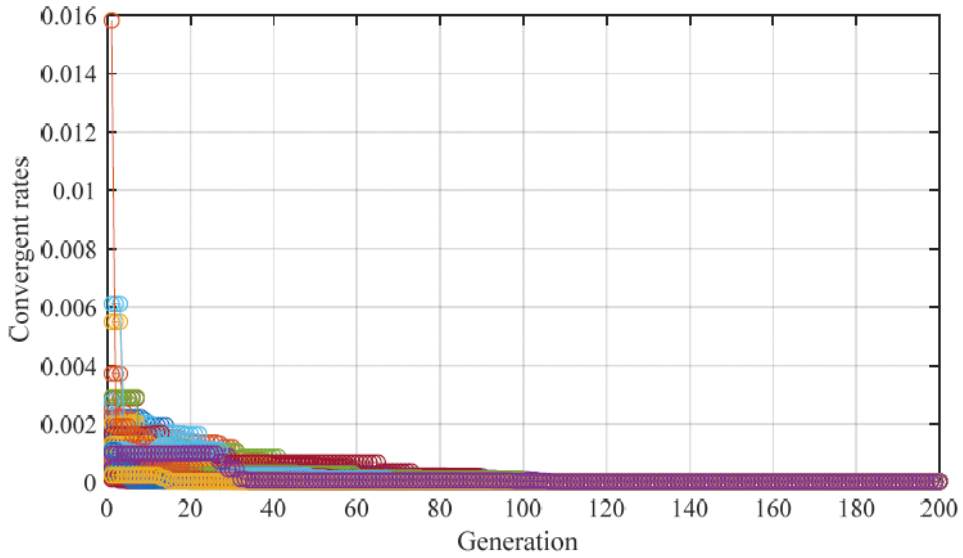

FIGURE 7. Convergent rates of cooperative FPA-ATS based FOPID design optimization for LFC system with non-reheated turbine

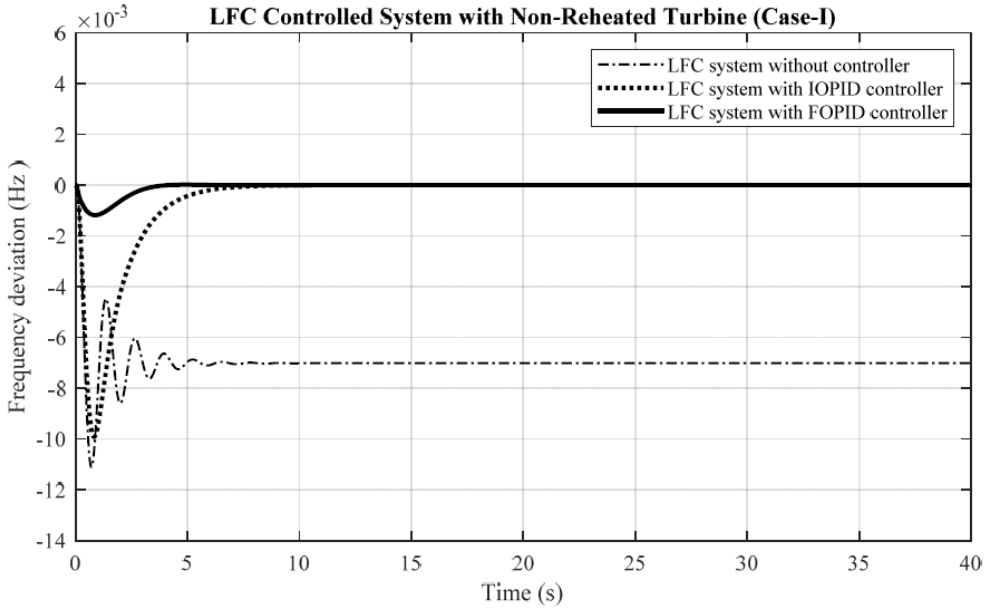

FIGURE 8. Responses of LFC system without and with IOPID and FOPID controllers optimized by FPA-ATS (case-I: non-reheated turbine)

then summarized in Table 5. It can be noticed that the FOPID controller can give much less damping and faster recovering than the IOPID controller.

5.2. **Case-II: LFC with reheated turbine.** For a reheated turbine, the model parameters are employed as follows [49]: $K_m = 120$, $T_m = 20$ s, $T_t = 0.3$ s, $T_g = 0.08$ s, $R = 2.4$, $T_r = 4.20$ s and $c = 0.35$. From Figure 7, the plant model, $G_p(s)$, is stated in (20).

$$\begin{aligned} G_p(s)|_{reheated\text{-}turbine} &= \frac{G_g G_t G_m}{1 + (G_g G_t^{reheated} G_m)/R} \\ &= \frac{87.5s + 59.52}{s^4 + 16.12s^3 + 46.24s^2 + 48.65s + 25.3} \end{aligned} \tag{20}$$

With the cooperative FPA-ATS based design optimization, the IOPID and FOPID controllers for the LFC system with a reheated turbine are optimized as stated in (21) and (22), respectively. The convergent rates of this case are omitted because they have a similar form to that of the case-I in Figure 7. Responses of the LFC controlled system with a reheated turbine when a load disturbance $\Delta P_d = 0.01$ p.u.MW is applied are plotted in Figure 9.

$$G_c(s)|_{IOPID} = 2.8137 + \frac{1.2543}{s} + 0.7786s \tag{21}$$

$$G_c(s)|_{FOPID} = 8.8519 + \frac{5.6134}{s^{0.9982}} + 2.9178s^{0.9814} \tag{22}$$

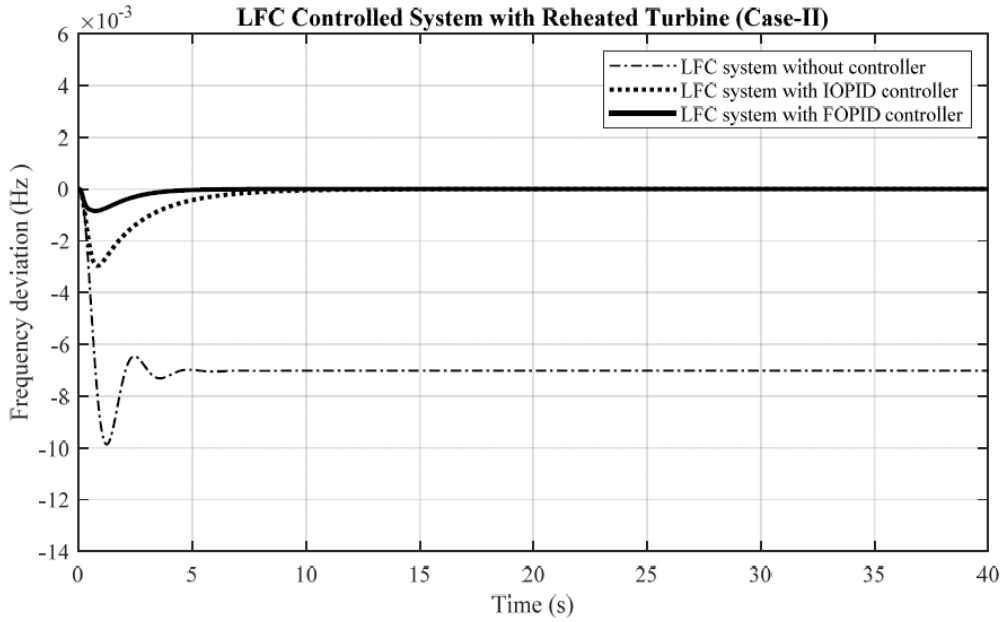

FIGURE 9. Responses of LFC system without and with IOPID and FOPID controllers optimized by FPA-ATS (case-II: reheated turbine)

From Figure 9, it can be observed that both IOPID and FOPID controllers can improve the damping of the LFC system with a reheated turbine. Results obtained for case-II are also summarized in Table 5. In this case, the FOPID controller can also yield much less damping and faster recovering than the IOPID controller.

5.3. **Case-III: LFC with hydro turbine.** For a hydro turbine, the model parameters are utilized as follows [49]: $K_m = 1$, $T_m = 6$ s, $T_h = 4$ s, $T_g = 0.2$ s and $R = 0.05$. The plant model, $G_p(s)$, is stated in (23). For this case, it can be considered as the hard-to-be-controlled plant because it is inherently unstable.

$$G_p(s)|_{hydro\text{-}turbine} = \frac{G_g G_t G_m}{1 + (G_g G_t^{hydro} G_m)/R} = \frac{-1.667s + 0.4167}{s^3 + 5.667s^2 - 29.92s + 8.75} \tag{23}$$

With the cooperative FPA-ATS based design optimization, the IOPID and FOPID controllers for the LFC system with a hydro turbine are optimized as stated in (24) and (25), respectively. The convergent rates of this case are omitted because they have a similar form to that of the case-I in Figure 7. Responses of the LFC controlled system with a hydro turbine once a load disturbance $\Delta P_d = 0.01$ p.u.MW is applied are depicted

in Figure 10.

$$G_c(s)|_{IOPID} = -17.9652 + \frac{0.1544}{s} + 1.8126s \tag{24}$$

$$G_c(s)|_{FOPID} = -18.7214 + \frac{0.1978}{s^{0.9982}} + 2.2969s^{0.9965} \tag{25}$$

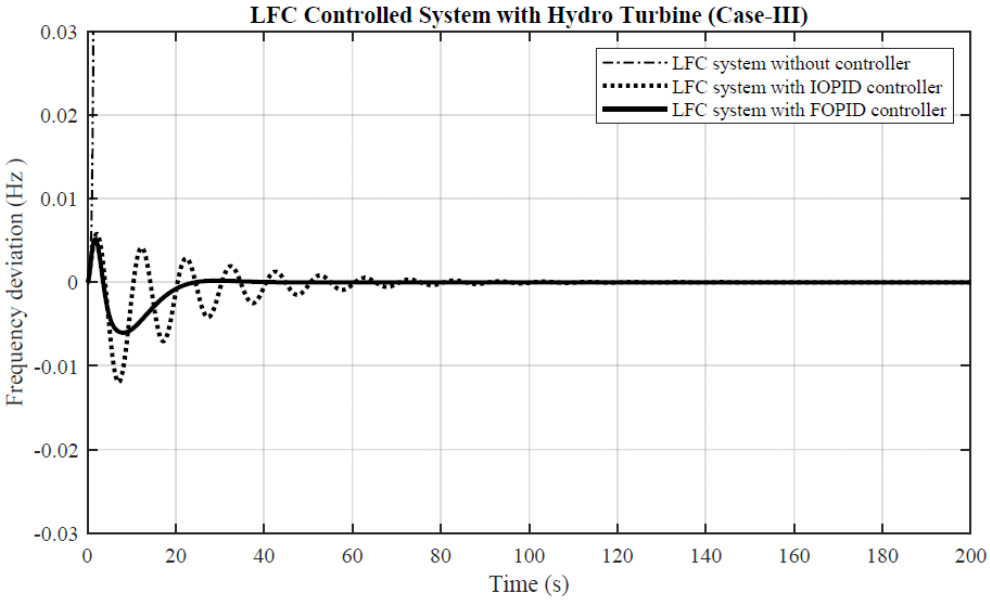

FIGURE 10. Responses of LFC system without and with IOPID and FOPID controllers optimized by FPA-ATS (case-III: hydro turbine)

From Figure 10, it can be observed that both IOPID and FOPID controllers can stabilize and improve the damping of the LFC system with a hydro turbine. Results obtained for case-III are then summarized in Table 5. Also, the FOPID controller in this case can provide much less damping and faster recovering than the IOPID controller.

TABLE 5. Comparison results of IOPID and FOPID controllers designed by cooperative FPA-ATS for LFC systems

Controllers	LFC system responses								
	Case-I (non-reheated turbine)			Case-II (reheated turbine)			Case-III (hydro turbine)		
	PO_{reg}(%)	t_{reg}(s)	e_{ss}(%)	PO_{reg}(%)	t_{reg}(s)	e_{ss}(%)	PO_{reg}(%)	t_{reg}(s)	e_{ss}(%)
without	63.40	8.26	0.70	42.47	6.75	0.72	——unstable——		
IOPID	1.03	7.44	0.00	0.31	7.25	0.00	1.24	49.62	0.01
FOPID	0.11	2.88	0.00	0.08	3.67	0.00	0.68	22.19	0.00

6. **Conclusions.** A novel serial-heterogeneous cooperative metaheuristic optimization algorithm denoted as the cooperative FPA-ATS algorithm has been proposed in this paper. The proposed cooperative FPA-ATS algorithm has been formed from the ATS, one of the trajectory-based metaheuristic optimization techniques possessing the dominant exploitative property, and the FPA, one of the most efficient population-based metaheuristic optimization techniques having the dominant explorative property. The search performance of the cooperative FPA-ATS compared with the ATS and FPA have been elaborately tested against ten selected benchmark functions. Superiority of the cooperative FPA-ATS's search performance to the ATS and FPA have been reported in this paper. Then, the cooperative FPA-ATS algorithm has been applied to designing the optimal

FOPID controllers for the LFC systems with three types of turbines. Based on modern optimization, results obtained have shown that the proposed cooperative FPA-ATS algorithm could successfully provide the optimal FOPID controllers for the considered LFC systems according to the design specifications and search bounds of all types of turbines. Once compared with the IOPID controller, it could be noticed that the FOPID could yield very satisfactory response with less damping and faster recovering than the IOPID.

REFERENCES

[1] F. Glover and G. A. Kochenberger, *Handbook of Metaheuristics*, Kluwer Academic Publishers, 2003.

[2] E. G. Talbi, *Metaheuristics from Design to Implementation*, John Wiley & Sons, 2009.

[3] T. Ganesan, P. Vasant and I. Elamvazuthi, *Advances in Metaheuristics: Applications in Engineering Systems*, CSC Press, Taylor & Francis Group, 2017.

[4] X. S. Yang, *Engineering Optimization: An Introduction with Metaheuristic Applications*, John Wiley & Sons, 2010.

[5] S. Dash, B. K. Tripathy and A. U. Rahman, *Handbook of Research on Modeling, Analysis, and Application of Nature-Inspired Metaheuristic Algorithms (Advances in Computational Intelligence and Robotics)*, IGI Global Engineering Science Reference, 2018.

[6] S. Sujitjorn, T. Kulworawanichpong, D. Puangdownreong and K.-N. Areerak, Adaptive tabu search and applications in engineering design, in *Integrated Intelligent Systems for Engineering Design*, X. F. Zha and R. J. Howlett (eds.), Netherland, IOS Press, 2006.

[7] F. Glover, Tabu search – Part I, *ORSA Journal on Computing*, vol.1, no.3, pp.190-206, 1989.

[8] F. Glover, Tabu search – Part II, *ORSA Journal on Computing*, vol.2, no.1, pp.4-32, 1990.

[9] D. Puangdownreong, K.-N. Areerak, A. Srikaew, S. Sujitjorn and P. Totarong, System identification via adaptive tabu search, *Proc. of the IEEE International Conference on Industrial Technology (ICIT'02)*, vol.2, pp.915-920, 2002.

[10] T. Kulworawamichpong, K.-L. Areerak, K.-N. Areerak, P. Pao-la-or, D. Puangdownreong and S. Sujitjorn, Dynamic parameter identification of induction motors using intelligent search techniques, *Proc. of the 24th IASTED International Conference on Modelling, Identification, and Control (MIC2005)*, pp.328-332, 2005.

[11] D. Puangdownreong, K.-N. Areerak, K.-L. Areerak, T. Kulworawanichpong and S. Sujitjorn, Application of adaptive tabu search to system identification, *Proc. of the 24th IASTED International Conference on Modelling, Identification, and Control (MIC2005)*, pp.178-183, 2005.

[12] D. Puangdownreong and S. Sujitjorn, Image approach to system identification, *WSEAS Transactions on Systems*, vol.5, no.5, pp.930-938, 2006.

[13] S. Udomsuk, T. Areerak, K.-L. Areerak and K.-N. Areerak, Power loss identification of separately excited DC motor using adaptive tabu search, *European Journal of Scientific Research*, vol.60, no.4, pp.488-497, 2011.

[14] D. Puangdownreong, T. Kulworawanichpong and S. Sujitjorn, Input weighting optimization for PID controllers based on the adaptive tabu search, *Proc. of the International Conference of IEEE-TENCON 2004*, 2004.

[15] D. Puangdownreong, C. U-Thaiwasin and S. Sujitjorn, Optimized performance of a 2-mass rotary system using adaptive tabu search, *WSEAS Transactions on Circuits and Systems*, vol.3, no.5, pp.339-345, 2006.

[16] D. Puangdownreong and S. Sujitjorn, Obtaining an optimum PID controller via adaptive tabu search, *Lecture Notes in Computer Science*, vol.4432, pp.747-755, 2007.

[17] C. Thammarat, D. Puangdownreong and P. Sukserm, Design of PID controller with set-point weighting for process with time delay using adaptive tabu search, *Proc. of the 3rd Technology and Innovation for Sustainable Development International Conference (TISD2010)*, pp.194-199, 2010.

[18] C. Thammarat, D. Puangdownreong, P. Sukserm and S. Suwannarongsri, Optimum industrial PID controller design for process with time delay via adaptive tabu search, *Proc. of the 29th IASTED International Conference on Modelling, Identification, and Control (MIC2010)*, pp.197-202, 2010.

[19] K.-N. Areerak, T. Kulworawanichpong and S. Sujitjorn, Moving towards a new era of intelligent protection through digital relaying in power systems, *Lecture Notes in Computer Science*, vol.3213, pp.1255-1261, 2004.

[20] T. Kulworawanichpong, K.-L. Areerak, K.-N. Areerak and S. Sujitjorn, Harmonic identification for active power filters via adaptive tabu search method, *Lecture Notes in Computer Science*, vol.3215, pp.687-694, 2004.

[21] A. Oonsivilai and P. Pao-la-or, Application of adaptive tabu search for optimum PID controller tuning AVR system, *WSEAS Transactions on Power Systems*, vol.3, no.6, pp.495-506, 2008.

[22] K. Chaijarurnudomrung, K.-N. Areerak and K.-L. Areerak, The controller design of three-phase controlled rectifier using an artificial intelligence technique, *European Journal of Scientific Research*, vol.62, no.3, pp.410-425, 2011.

[23] K. Chaijarurnudomrung, K.-N. Areerak, K.-L. Areerak and A. Srikaew, The controller design of three-phase controlled rectifier using an adaptive tabu search algorithm, *Proc. of the 8th Electrical Engineering/Electronics, Computer, Telecommunications and Information Technology (ECTI-CON2011)*, pp.605-608, 2011.

[24] N. Sriyingyong and K. Attakitmongcol, Waveletet-based audio watermarking using adaptive tabu search, *Proc. of the 1st International Symposium on Wireless Pervasive Computing*, pp.1-5, 2006.

[25] D. Puangdownreong, S. Sujitjorn and T. Kulworawanichpong, Convergence analysis of adaptive tabu search, *ScienceAsia – Journal of the Science Society of Thailand*, vol.30, no.2, pp.183-190, 2004.

[26] D. Puangdownreong, T. Kulworawanichpong and S. Sujitjorn, Finite convergence and performance evaluation of adaptive tabu search, *Lecture Notes in Computer Science*, vol.3215, pp.710-717, 2004.

[27] T. Kulworawanichpong, D. Puangdownreong and S. Sujitjorn, Finite convergence of adaptive tabu search, *ASEAN Journal on Science and Technology for Development*, vol.21, nos.2&3, pp.103-115, 2004.

[28] X. S. Yang, Flower pollination algorithm for global optimization, *Unconventional Computation and Natural Computation, Lecture Notes in Computer Science*, vol.7445, pp.240-249, 2012.

[29] A. Abdelaziz, E. Ali and S. A. Elazim, Combined economic and emission dispatch solution using flower pollination algorithm, *International Journal of Electrical Power and Energy Systems*, vol.80, pp.264-274, 2016.

[30] A. Abdelaziz, E. Ali and S. A. Elazim, Implementation of flower pollination algorithm for solving economic load dispatch and combined economic emission dispatch problems in power systems, *Energy*, vol.101, pp.506-518, 2016.

[31] E. Emary, H. M. Zawbaa, A. E. Hassanien and B. Parv, Multi-objective retinal vessel localization using flower pollination search algorithm with pattern search, *Advances in Data Analysis and Classification*, vol.11, no.3, pp.611-627, 2017.

[32] S. Ouadfel and A. Taleb-Ahmed, Social spiders optimization and flower pollination algorithm for multilevel image thresholding: A performance study, *Expert Systems with Applications*, vol.55, pp.566-584, 2016.

[33] M. Sharawi, E. Emary, I. A. Saroit and H. El-Mahdy, Flower pollination optimization algorithm for wireless sensor network lifetime global optimization, *International Journal of Soft Computing and Engineering*, vol.4, no.3, pp.54-59, 2014.

[34] F. Hajjej, R. Ejbali and M. Zaied, An efficient deployment approach for improved coverage in wireless sensor networks based on flower pollination algorithm, *Computer Science and Information Technology*, pp.117-129, 2016.

[35] S. Suwannarongsri and D. Puangdownreong, Optimal solving large scale traveling transportation problems by flower pollination algorithm, *WSEAS Transactions on Systems and Control*, vol.14, pp.19-24, 2019.

[36] S. M. Nigdeli, G. Bekdao and X. S. Yang, Application of the flower pollination algorithm in structural engineering, *Metaheuristics and Optimization in Civil Engineering*, pp.25-42, 2016.

[37] O. K. Meng, O. Pauline, S. C. Kiong, H. A. Wahab and N. Jafferi, Application of modified flower pollination algorithm on mechanical engineering design problem, *Materials Science and Engineering*, vol.165, pp.012-032, 2017.

[38] D. Puangdownreong, Fractional order PID controller design for DC motor speed control system via flower pollination algorithm, *ECTI Transactions on Electrical Engineering, Electronics, and Communications*, vol.17, no.1, pp.14-23, 2019.

[39] T. Niyomsat and D. Puangdownreong, Optimal PIDA load frequency controller design for power systems via flower pollination algorithm, *WSEAS Transactions on Power Systems*, vol.14, pp.1-7, 2019.

[40] N. Pringsakul, D. Puangdownreong, C. Thammarat and S. Hlangnamthip, Obtaining optimal PIDA controller for temperature control of electric furnace system via flower pollination algorithm, *WSEAS Transactions on Systems and Control*, vol.14, pp.1-7, 2019.

[41] D. Puangdownreong, Optimal state-feedback design for inverted pendulum system by flower pollination algorithm, *International Review of Automatic Control*, vol.9, no.5, pp.289-297, 2016.
[42] X. He, X. S. Yang, M. Karamanoglu and Y. Zhao, Global convergence analysis of the flower pollination algorithm: A discrete time Markov chain approach, *Proc. of the International Conference on Computational Science (ICCS2017)*, pp.1354-1363, 2017.
[43] E. G. Talbi, A taxonomy of hybrid metaheuristics, *Journal of Heuristics*, vol.8, pp.541-564, 2002.
[44] M. El-Abd and M. Kamel, A taxonomy of cooperative search algorithms, *Lecture Notes in Computer Science*, vol.3636, pp.32-41, 2005.
[45] M. M. Ali, C. Khompatraporn and Z. B. Zabinsky, A numerical evaluation of several stochastic algorithms on selected continuous global optimization test problems, *Journal of Global Optimization*, vol.31, pp.635-672, 2005.
[46] M. Jamil and H.-J. Zepernick, Test functions for global optimization: A comprehensive survey, in *Swarm Intelligence and Bio-Inspired Computation: Theory and Applications*, X. S. Yang et al. (eds.), Elsevier Inc., 2013.
[47] P. Kundur, *Power System Stability and Control*, McGraw-Hill, New York, 1994.
[48] H. Shayeghi, H. A. Shayanfar and A. Jalili, Load frequency control strategies: A state-of-the-art survey for the researcher, *Energy Conversion and Management*, vol.50, pp.344-353, 2009.
[49] W. Tan, Unified tuning of PID load frequency controller for power systems via IMC, *IEEE Transactions on Power Systems*, vol.25, no.1, pp.341-350, 2010.
[50] W. Budiharto, E. Irwansyah, J. S. Suroso and A. A. S. Gunawan, Design of object tracking for military robot using PID controller and computer vision, *ICIC Express Letters*, vol.14, no.3, pp.289-294, 2020.
[51] I. Podlubny, *Fractional-Order Systems and Fractional-Order Controllers*, UEF-03-94, Slovak Academy of Sciences, Kosice, 1994.
[52] I. Podlubny, Fractional-order systems and $PI^{\lambda}D^{\mu}$-controllers, *IEEE Transactions on Automatic Control*, vol.44, no.1, pp.208-214, 1999.
[53] D. Puangdownreong, Optimal $PI^{\lambda}D^{\mu}$ controller design based on spiritual search for wind turbine systems, *International Journal of Innovative Computing, Information and Control*, vol.15, no.6, pp.2259-2273, 2019.
[54] C. Thammarat and D. Puangdownreong, CS-based optimal $PI^{\lambda}D^{\mu}$ controller design for induction motor speed control system, *International Journal on Electrical Engineering and Informatics*, vol.11, no.4, pp.638-661, 2019.
[55] S. Sumpunsri and D. Puangdownreong, Multiobjective Lévy-flight firefly algorithm for optimal PIDA controller design, *International Journal of Innovative Computing, Information and Control*, vol.16, no.1, pp.173-187, 2020.
[56] T. Jitwang and D. Puangdownreong, Application of cuckoo search to robust PIDA controller design for liquid-level system, *International Journal of Innovative Computing, Information and Control*, vol.16, no.1, pp.189-205, 2020.
[57] K. Lurang and D. Puangdownreong, Two-degree-of-freedom PIDA controllers design optimization for liquid-level system by using modified bat algorithm, *International Journal of Innovative Computing, Information and Control*, vol.16, no.2, pp.715-732, 2020.
[58] A. Tepljakov, F. Petlenkov and J. Belikov, FOMCON: A MATLAB toolbox for fractional-order system identification and control, *International Journal of Microelectronics and Computer Science*, vol.2, no.2, pp.51-62, 2011.